The Cu-Nd (Copper-Neodymium) System

By P.R. Subramanian and D.E. Laughlin
Carnegie Mellon University

Equilibrium Diagram

The equilibrium phases of the Cu-Nd system are: (1) the liquid, L, without any miscibility gaps; (2) the fcc terminal solid solution, (Cu), with negligible solid solubility of Nd in (Cu); (3) the Nd-rich bcc terminal solid solution, (βNd), based on the equilibrium phase of pure Nd between 863 and 1021 °C (the solid solution of Cu in (βNd) is negligible); (4) the Nd-rich dcph terminal solid solution (αNd), stable below 863 °C, with negligible solid solubility of Cu in (αNd); (5) the orthorhombic intermediate phase, Cu_6Nd, stable up to the congruent melting temperature of 910 °C; (6) the hexagonal phase, Cu_5Nd, stable up to the peritectic temperature of 870 °C; (7) Cu_7Nd_2, with unknown structure, existing within the limited temperature range 785 to 825 °C; (8) the orthorhombic phase, Cu_4Nd, stable up to the peritectic temperature of 845 °C; (9) the orthorhombic phase, Cu_2Nd, stable up to the congruent melting temperature of 840 °C; and (10) the most Nd-rich intermediate phase, CuNd, stable up to the peritectic melting temperature of 675 °C.

[83Car] and [83Che] independently investigated the Cu-Nd system, and more recently, [84Lak] examined the Cu-rich side. The three reports are in agreement with regard to the existence of the five intermediate phases. The phase diagrams of [83Car] and [83Che] were established on the basis of differential thermal analysis (DTA), metallography, and X-ray analysis, whereas [84Lak] used scanning electron microscopy with energy-dispersive analysis in addition to the above mentioned techniques. [83Car] carried out several thermal cycles with varying cooling rates to determine the various thermal arrests. On the other hand, the phase diagram proposed by [84Lak] is tentative, because only a limited number of data points were obtained; however, in the Cu-rich side, this phase diagram is in general agreement with that of [83Car].

Fig. 1 Assessed Cu-Nd Phase Diagram

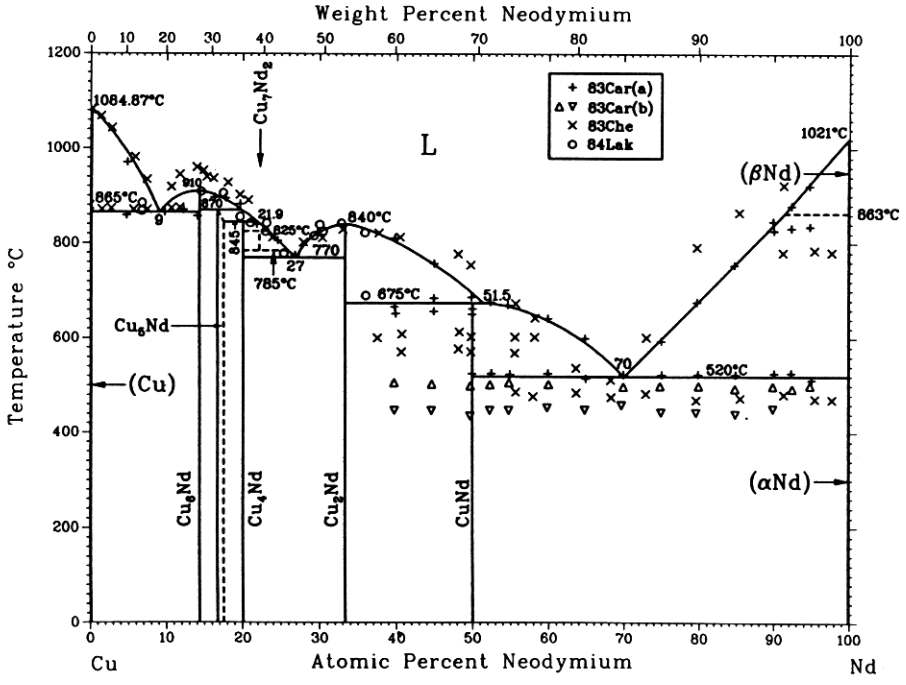

(a) Liquidus and invariant temperatures. (b) Thermal effects observed on heating (Δ) and on cooling (▽).
P.R. Subramanian and D.E. Laughlin, 1988.

Fig. 2 Enlargement of Cu-Nd Phase Diagram in the Vicinity 5 to 35 at.% Nd

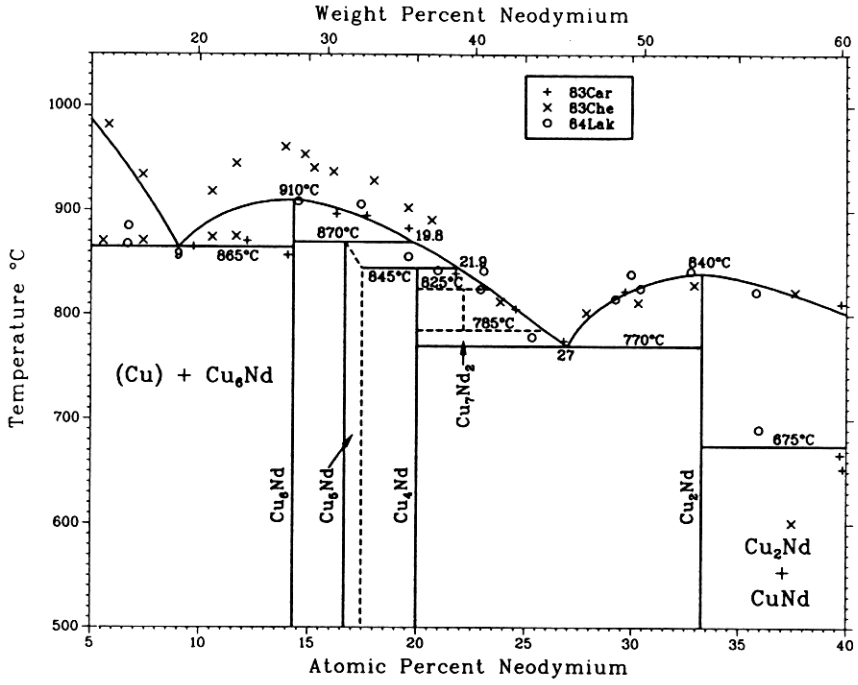

P.R. Subramanian and D.E. Laughlin, 1988.

As a result, the assessed phase diagram, shown in Fig. 1, has been derived primarily from the data of [83Car]. Minor modifications have been made in the liquidus in the vicinity of the two congruent points at 910 and 840 °C to conform to thermodynamic rules for construction of congruent inflection points [81Goo].

In addition to the assessed phase diagram, Fig. 1 shows the composite of all available data. In the interest of clarity, invariant data points have been omitted in the vicinity of 15 to 35 at.% Nd. Figure 2 shows an enlarged version of the Cu-Nd equilibrium diagram in the region 5 to 35 at.% Nd and includes all available data from [83Car], [83Che], as well as [84Lak].

Terminal Solid Solubility

[83Car] concluded that the solid solubility of Cu in (αNd) is negligible because the lattice parameters of (αNd) do not change significantly on alloying with Cu. Similarly, there is no evidence of any terminal solid solubility at the Cu-rich end.

Liquidus and Solidus

Experimental data for the Cu-Nd liquidus boundaries are listed in Table 1. The melting points of (Cu) and (βNd) are accepted as 1084.87 °C [Melt] and 1021 °C [78Bea, 86Gsc], respectively. The melting point of (βNd), as reported by [83Che], is substantially higher than the accepted melting point, and similarly, their liquidus on the Nd-rich side shows a shift toward higher temperatures. In contrast, their eutectic horizontal in the Nd-rich side shows a deviation in the opposite direction, and is about 40 °C lower than the data of [83Car].

The accepted (αNd) ↔ (βNd) transition temperature of 863 °C, taken from [78Bea] and [86Gsc], is well above the values reported by both [83Car] and [83Che]. [83Che] attributed the lower value of the α ↔ β transition temperature to the presence of impurities in the Nd metal. However, according to [83Car], the α ↔ β transition temperature is not altered from its elemental value by the addition of Cu. According to the present authors, the transformation is most likely to take place through a catatectic reaction and at temperatures very close to that for elemental Nd, in view of the low solubility of Cu in Nd. Similar behavior has been observed in the Cu-Ce system (this issue). [83Car] reported the occurrence of a thermal effect below the eutectic temperature of 520 °C and between 40 and 100 at.% Nd. The thermal effect was observed at 500 to 510 °C on heating and at 450 °C on cooling, and [83Car] suggested that a first-order transformation occurs in this region. No such transformations were reported by [83Che].

On the Cu-rich side, the liquidus boundaries of [83Car] and [84Lak] are in good accord. However, the liquidus boundary of [83Che] lies at temperatures well above those of [83Car]. This might be due to the fact that the thermal arrest data of [83Che] are based on heating cycles, and as such, are likely to show some superheating effects.

Table 2 summarizes the various invariant reactions reported for the Cu-Nd system. The three eutectic reactions occurring in the Cu-Nd system are:

- The liquid of composition 9 at.% Nd, in equilibrium with (Cu) and Cu_6Nd at 865 °C. The eutectic temperature is from [83Car] and is within 10 °C of the values reported by [83Che] and [84Lak]. The eutectic composition represents a compromise between the data of [83Car], [83Che], and [84Lak].
- The liquid of composition 27 at.% Nd, in equilibrium with Cu_4Nd and Cu_2Nd at 770 °C.
- The liquid of composition 70 at.% Nd, in equilibrium with CuNd and (αNd) at 520 °C. The accepted eutectic temperature and composition are from [83Car]. According to [83Che], the eutectic lies at 67 at.% Nd and at a much lower temperature of 478 °C. The data of [83Car] were accepted because they are closer to the general trend observed for the eutectic temperatures in the Cu-lanthanide systems (see "The Copper-Rare Earth Systems," in this issue).

Intermediate Phases

Of the five intermediate phases, Cu_6Nd and Cu_2Nd melt congruently, and the others decompose through peritectic reactions.

There is a large disparity in the melting points reported for Cu_6Nd by [83Car] and [83Che]. The accepted melting temperature of 910 °C is taken from [83Car] and is very close to that reported by [84Lak].

The phase Cu_5Nd was reported by [83Car] to have a homogeneity range, and the accepted melting point of 870 °C from [83Car] agrees with the systematics observed for the melting behavior of the other lanthanide 5-to-1 phases, whereas the data of [83Che] show Cu_5Nd melting at the much higher temperature of 916 °C. Although [84Lak] reported that Cu_5Nd melts at 847 °C, their data show the presence of thermal arrests at temperatures close to 870 °C, closer to the accepted melting point of Cu_5Nd. If this is the case, then the thermal arrests reported by [84Lak] in the vicinity of 847 °C can be attributed to the melting temperature of Cu_4Nd, in concurrence with the accepted value of 840 °C from [83Car].

[83Car] reported the high-temperature formation of Cu_7Nd_2 at 825 °C, with its subsequent decomposition at 785 °C. This phase could not be retained at room temperature under any circumstances. The presence of Cu_7Nd_2 is not corroborated by either [83Che] or [84Lak], although the diagram of [84Lak] indicates the presence of thermal arrests near 830 °C as well as near 785 °C. Therefore, it is possible that Cu_7Nd_2 exists only within a limited temperature range.

Cu_2Nd melts congruently at 830 °C. The data are from [83Car], and in this instance, the accepted melting point is in good agreement with both [83Che] and [84Lak].

CuNd decomposes peritectically at 670 °C. The melting temperature is from [83Car] and agrees with the systematics for the Cu-lanthanide systems. In addition, [83Car] reported thermal effects at 650 to 660 °C and between 450 and 500 °C in the region 40 to 50 at.% Nd and suggested that these might be due to modifications in the crystal structure of CuNd. [83Car] concluded that the behavior of CuNd is intermediate between that of the lighter lanthanide phases with Cu and that of the corresponding heavy lanthanide

Table 1 Cu-Nd Experimental Liquidus Data

Composition, at.% Nd	Temperature, °C	Composition, at.% Nd	Temperature, °C
[83Car](a)			
5.0	970	45.0	758
10.0	865	50.0	685
12.5	895	52.5	675
14.3	910	55.0	668
16.7	895	60.0	638
18.3	893	65.0	590
20.0	880	70.0	520
22.2	840	75.0	590
25.0	803	80.0	675
27.0	770	85.0	755
30.0	820	90.0	840
33.3	840	92.5	878
40.0	810	95.0	920
[83Che](b)			
0.44	1082	28.10	800
1.80	1068	30.59	813
3.21	1044	33.33	830
6.18	980	37.83	818
7.74	932	40.80	813
11.05	918	48.36	777
12.22	944	50.00	754
14.29	962	55.64	670
15.25	953	58.25	640
15.88	940	63.80	534
16.67	936	68.27	510
18.50	928	73.02	600
20.00	900	79.86	790
21.26	890	85.41	864
24.19	810	91.36	920
[84Lak](c)			
7.2	885	25.7	779
14.9	910	29.7	815
17.9	908	30.3	840
20.0	858	30.9	824
21.3	846	33.3	843
23.3	842	36.2	823
23.3	829		

(a) Compositions and temperatures refer to the data points given in the phase diagram of [83Car]. (b) Liquidus data are as reported by [83Che]. (c) Compositions and temperatures refer to the data points given in the tentative diagram of [84Lak].

Table 2 Special Points of the Assessed Cu-Nd Phase Diagram

Reaction	Compositions of the respective phases, at.% Nd			Temperature, °C	Reaction type	Reference
(Cu) ↔ L		0.0		1084.87	Melting point	[Melt]
L ↔ (Cu) + Cu_6Nd	10	0	14.3	865	Eutectic	[83Car]
	9	0	14.3	874		[83Che]
	8	0	14.3	868		[84Lak]
	9	**0**	**14.3**	**865**		(a)
L ↔ Cu_6Nd		**14.3**		**910**	Congruent	[83Car]
		14.3		917		[83Che]
		14.3		962		[84Lak]
L + Cu_6Nd ↔ Cu_5Nd	20.5	14.3	16.7	870	Peritectic	[83Car]
	19	14.3	16.7	916		[83Che]
	20.9	14.3	**16.7**	847		[84Lak]
	19.8	**14.3**	16.7	**870**		(a)
L + Cu_5Nd ↔ Cu_4Nd	23.0	16.7	20.0	845	Peritectic	[83Car]
	23.0	16.7	20.0	853		[83Che]
	25.3	16.7	20.0	829		[84Lak]
	21.9	**16.7**	**20.0**	**845**		(a)
L ↔ Cu_4Nd + Cu_2Nd	**27.0**	**20.0**	**33.3**	**770**	Eutectic	[83Car]
	26.0	20.0	33.3	760		[83Che]
	28.0	20.0	33.3	785		[84Lak]
L ↔ Cu_2Nd		**33.3**		**840**	Congruent	[83Car]
		33.3		830		[83Che]
		33.3		843		[84Lak]
L + Cu_2Nd ↔ CuNd	**51.5**	**33.3**	**50.0**	**675**	Peritectic	[83Car]
	60.0	33.3	50.0	602		[83Che]
	?	33.3	50.0	691		[84Lak](b)
L ↔ CuNd + (αNd)	**70**	**50**	**100**	**520**	Eutectic	[83Car]
	67	50	100	478		[83Che]
(βNd) ↔ L + (αNd)	100	90.0	100	830	Catatectic	[83Car]
	100	81.6	100	780		[83Che]
	~100	**<91.5**	**~ 100**	**<863**		(a)
(αNd) ↔ (βNd)		100		863	Allotropic	[78Bea, 86Gsc]
(βNd) ↔ L		100		1021	Melting point	[78Bea, 86Gsc]

Note: Selected values for the assessed phase diagram are shown in boldface type.
(a) From the assessed phase diagram. **(b)** Estimated from the incomplete phase diagram of [84Lak].

phases. The equiatomic phases CuLa, CuCe, and CuPr crystallize with an orthorhombic structure, whereas the rest of the lanthanide phases crystallize with a cubic structure. According to [83Car], the thermal data suggest that CuNd crystallizes in both forms, with the cubic structure predominant at elevated temperatures. This is also corroborated by resistivity and lattice parameter measurements, which show sudden changes in the region 450 to 510 °C. In contrast, [83Che] reported the melting of CuNd at 602 °C, with a solid-state transformation occurring at 574 °C. Therefore, although the existence of a solid state transformation has been confirmed, there is an uncertainty with regard to the precise temperature of transformation.

Crystal Structures and Lattice Parameters

The experimental values for the lattice parameters of the five Cu-Nd intermediate phases are listed in Table 3. The accepted lattice parameter data, crystal structures, and related parameters for the various phases are summarized in Tables 4 and 5.

From X-ray diffraction data, [70Bus] confirmed that Cu_6Nd crystallizes with the orthorhombic $CeCu_6$ prototype structure; lattice parameter data of [70Bus] and [83Car] are in good agreement.

Cu_5Nd has the hexagonal $CaCu_5$ structure, and lattice parameter data reported for this phase by various authors are in excellent agreement.

From X-ray investigation, [80Pop] concluded that Cu_4Nd is isostructural with $CeCu_4$ and crystallizes with an orthorhombic structure. In contradiction, [83Car] reported that Cu_4Nd forms with a fcc sub-cell. Cu_4RE phases with an orthorhombic structure have been reported for RE = Ce and RE = Pr (see Ce-Cu and Cu-Pr, in this issue), and the data of [80Pop] have been accepted in Tables 4 and 5.

Cu_2Nd has the orthorhombic $CeCu_2$ structure, and lattice parameters reported for this phase by [63Sto],

Table 3 Cu-Nd Experimental Lattice Parameters

Phase	Crystal structure	Lattice parameters, nm a	b	c	Reference
Cu_6Nd	Orthorhombic	0.8092	0.5062	1.0105	[70Bus](a)
		0.8064	0.5058	1.0113	[83Car](b)
		0.7952	0.5044	1.0203	[84Lak](a)
Cu_5Nd	Hexagonal	0.5104	...	0.4107	[59Wer](c)
		0.5110	...	0.4107	[61Dwi](e)
		0.5110	...	0.4104	[71Bus](a)
		0.5105	...	0.4113	[80Pop](d)
		0.5101	...	0.4108	[83Car](b)
		0.5097	...	0.4112	[84Lak](a)
Cu_4Nd	Orthorhombic	0.450	0.806	0.915	[80Pop](d)
	Cubic	0.527	...	...	[83Car](e)
Cu_2Nd	Orthorhombic	0.4387	0.7059	0.7420	[63Sto](c)
		0.4387	0.7001	0.7418	[83Car](b)
		0.4384	0.7096	0.7417	[84Lak](a)
CuNd	Orthorhombic	0.722	0.427	0.626	[65Wal](d)
		0.732	0.455	0.559	[65Dwi](d)
		0.7279	0.4514	0.5634	[83Car](b)
		0.7302	0.4569	0.5578	[84Lak](a)

(a) Alloys prepared from 99.99% pure Cu and 99.9% pure Nd. (b) Alloys made from 99.999% pure Cu and 99.9% pure Nd. (c) Alloys made from 99.999% pure Cu and 99+% pure Nd. (d) Alloy purity not given. (e) Reported by [83Car] to have an fcc subcell.

Table 4 Cu-Nd Crystal Structure Data

Phase	Composition, at.% Nd	Pearson symbol	Space group	Strukturbericht designation	Prototype
(Cu)	0	*cF*4	$Fm\bar{3}m$	*A*1	Cu
Cu_6Nd	~14.29	*oP*28	*Pnma*	...	$CeCu_6$
Cu_5Nd	~16.67	*hP*6	*P*6/*mmm*	$D2_d$	$CaCu_5$
Cu_4Nd	~20.0	*oP*20	*Pnnm*	...	$CeCu_4$
Cu_2Nd	~33.3	*oI*12	*Imma*	...	$CeCu_2$
CuNd	~50	*oP*8	*Pnma*	*B*27	FeB
(βNd)	100	*cI*2	$Im\bar{3}m$	*A*2	W
(αNd)	100	*hP*4	$P6_3/mmc$	*A*3′	(αLa)

[83Car], and [84Lak] are given in Table 3, along with the reported purity of the starting materials. The data of [83Car] are accepted in Tables 4 and 5, because of their consistency with the systematics of other 1-to-2 Cu-lanthanide phases.

The equiatomic phase CuNd is the most Nd-rich phase in the Cu-Nd system, and it crystallizes with the orthorhombic FeB structure. As seen in Table 3, the lattice parameters reported by [65Dwi] and [65Wal] are in disagreement, with the unit cell volume calculated from the data of [65Dwi] lower than that obtained from the data of [65Wal]. A similar disparity has been observed in the Cu-Pr system (in this issue), and in that instance, the data of [65Dwi] were accepted. In the Cu-Nd system, the same assumption is valid, because the results of [65Dwi] are corroborated by the more recent data of [83Car] and [84Lak]. Also, it has been shown that the formula unit volume of the equiatomic phases decreases linearly with decreasing trivalent ionic radii of the lanthanide element (see "The Copper-Rare Earth Systems," in this issue), and in Cu-Nd, the data of [65Dwi] show the best fit with this linear trend.

Thermodynamics

No experimental thermodynamic data are available for the Cu-Nd system. In the present modeling, therefore, the experimental Cu-Nd liquidus data were utilized to derive analytical expressions for the Gibbs energy function of the liquid, as well as the Gibbs energies of formation of the various Cu-Nd intermediate phases. The basic assumptions behind the modeling are discussed in earlier evaluations (see Cu-Ce and Cu-Pr, in this issue).

In the present evaluation, data for the two eutectic points at 9 at.% Nd, 865 °C and 70 at.% Nd, 520 °C were utilized for deriving the integral molar excess Gibbs energy of the liquid. The resultant expression for the integral Gibbs energy of the liquid is given in Table 6. The integral molar Gibbs energies of the intermediate phases were next derived by solving for equi-

Fig. 3 Assessed vs Calculated Cu-Nd Phase Diagram

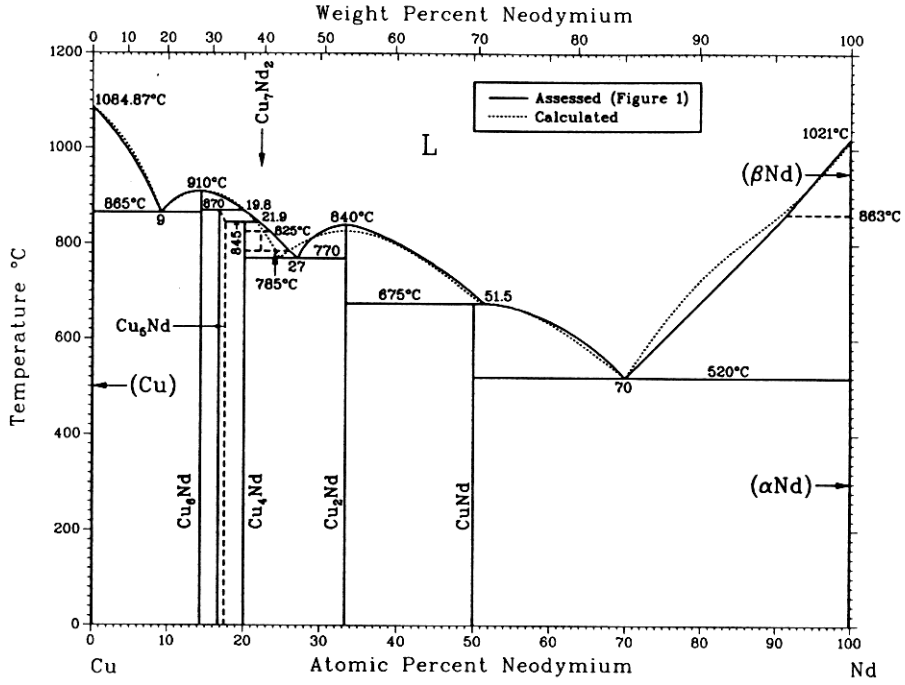

P.R. Subramanian and D.E. Laughlin, 1988.

Table 5 Cu-Nd Lattice Parameter Data

Phase	Composition, at.% Nd	Lattice parameters,nm a	b	c	Comment	Reference
(Cu)	0	0.36146	...	...	At 25 °C	[Massalski]
Cu_6Nd	~14.29	0.8078	0.5060	1.0109	...	[70Bus, 83Car]
Cu_5Nd	~16.67	0.5105	...	0.4109	...	(a)
Cu_4Nd	~20.0	0.450	0.806	0.915	...	[80Pop]
Cu_2Nd	~33.3	0.4387	0.7001	0.7418	...	[83Car]
CuNd	~50	0.7300	0.4544	0.5601	...	(b)
(βNd)	100	0.413	...	...	At 883 °C	[78Bea, 86Gsc]
(αNd)	100	0.36582	...	1.17966	At 24 °C	[78Bea, 86Gsc]

(a) [59Wer, 61Dwi, 71Bus, 80Pop, 83Car, 84Lak]. (b) [65Dwi, 83Car, 84Lak].

librium between the liquid and the respective intermediate phases at various invariant temperatures. The Gibbs energies of the phases at various temperatures were then fitted by least-squares analysis to give the analytic expressions that are listed in Table 6.

In order to assess the internal consistency of the Gibbs energy functions in Table 6, the liquidus boundaries were, in turn, generated from the Gibbs energy functions. The calculated phase boundaries, shown in Fig. 3, match reasonably well with the experimental liquidus, with some exceptions, however, in the Nd-rich end and in the vicinity of 27 to 50 at.% Nd. The calculated L/L + (αNd) liquidus at the Nd-rich end lies above the experimental liquidus. This deviation toward higher temperatures might be explained by the difference between the accepted α ↔ β transformation temperature and that reported by [83Car], whose liquidus boundary is reproduced in Fig. 3. On the other hand, the discrepancy in the region 27 to 50 at.% Nd is characteristic of the present modeling approach, which always gives a symmetrical liquidus on either side of a congruently melting intermediate phase. In this system, the Gibbs energy function for Cu_2Nd was evaluated from liquidus data at three invariant temperatures (770, 840, and 675 °C). The resultant eutectic composition at 770 °C is at ~24.5 at.% Nd and is accompanied by shifts of the Cu_4Nd + L/L liquidus and the L/L + Cu_2Nd liquidus toward higher Cu content. Alternately, the exclusion of the liquidus data at the congruent point gave the following expression for the Gibbs energy of Cu_2Nd:

Table 6 Cu-Nd Thermodynamic Properties

Lattice stability parameters for Cu(a)

$G^0(Cu, L) = 0$

$G^0(Cu, fcc) = -13\,054 + 9.613\,T$

Lattice stability parameters for Nd(b)

$G^0(Nd, L) = 0$

$G^0(Nd, bcc) = -7140 + 5.517\,T$

$G^0(Nd, dcph) = -10\,170 + 8.184\,T$

Integral molar Gibbs energies(c)

$G(L) = X(1-X)(-100\,593 + 61\,310\,X) + RT[X \ln X + (1-X) \ln (1-X)]$

$\Delta_f G(Cu_6Nd) = -25\,369 + 8.53\,T$

$\Delta_f G(Cu_5Nd) = -20\,749 + 3.29\,T$

$\Delta_f G(Cu_4Nd) = -18\,078 + 0.65\,T$

$\Delta_f G(Cu_2Nd) = -39\,059 + 14.07\,T$

$\Delta_f G(CuNd) = -32\,086 + 9.64\,T$

Note: Standard states: pure liquid Cu and pure liquid Nd. Gibbs energies are expressed in J/mol, and temperatures are in K. X is the atomic fraction of Nd. Mol refers to the atom as the elementary entity.
(a) From [Hultgren,E]. (b) From [83Cha]; melting point and transformation temperatures are from [78Bea] and [86Gsc]. (c) From the phase diagram [this work].

$\Delta_f G(Cu_2Nd) = -46\,833 + 22.04\,T$

The resultant Cu_2Nd + L/L liquidus and the L/L + Cu_2Nd liquidus, derived from the above expression, lie at temperatures that are well below that of the experimental liquidus, particularly in the vicinity of the congruent point. Because the uncertainty of the melting point of Cu_2Nd is smaller than the uncertainty of the eutectic composition at 770 °C, the original expression for the integral Gibbs energy of Cu_2Nd, as listed in Table 6, was chosen as being more consistent with the experimental data. In general, the Gibbs energy functions generated in the present modeling adequately reproduce the phase boundaries of the experimental equilibrium diagram.

The enthalpies of formation from the present modeling are compared in Table 7 with those derived on the basis of the semi-empirical model of Miedema [80Mie, 83Nie]. In all the cases, the Miedema values are more exothermic than those obtained in the present calculation.

Table 7 Calculated Enthalpies of Formation of the Cu-Nd Intermediate Phases vs Theoretical Estimates Based on Miedema's Model

Phase	Enthalpy of formation, kJ/mol: Present modeling	Miedema model(a)
Cu_6Nd	-25.4	-28.7
Cu_5Nd	-20.8	-31.2
Cu_4Nd	-18.1	-34.5
Cu_2Nd	-39.1	-43.5
CuNd	-32.1	-42.6

Note: Standard states are liquid Cu and liquid Nd.
(a) From [83Nie].

Cited References

59Wer: J.H. Wernick and S. Geller, "Transition Element-Rare Earth Compounds with the Cu_5Ca Structure," *Acta Crystallogr., 12,* 662-665 (1959). (Crys Structure; Experimental)

61Dwi: A.E. Dwight, "Factors Controlling the Occurrence of Laves Phases and AB_5 Compounds among Transition Elements," *Trans. ASM, 53,* 479-500 (1961). (Crys Structure; Experimental)

63Sto: A.R. Storm and K.E. Benson, "Lanthanide-Copper Intermetallic Compounds having the $CeCu_2$ and AlB_2 Structure," *Acta Crystallogr., 16,* 701-702 (1963). (Crys Structure; Experimental)

65Dwi: A.E. Dwight, R.A. Conner, Jr., and J. W. Downey, "Crystal Structures of Compounds of the Rare Earths with Cu, Ag, Au, and Ga," Proc. 5th Rare Earth Res. Conf., Aug 30-Sept 1, Ames, IA, *5,* 35-44 (1965). (Crys Structure; Experimental)

65Wal: R.E. Walline and W.E. Wallace, "Magnetic and Structural Characteristics of Lanthanide-Copper Compounds," *J. Chem. Phys., 42*(2), 604-607 (1965). (Crys Structure; Experimental)

70Bus: K.H.J. Buschow and A.S. van der Goot, "The Crystal Structure of Some Copper Compounds of the Type RCu_6," *J. Less-Common Met., 20,* 309-313 (1970). (Crys Structure; Experimental)

71Bus: K.H.J. Buschow and A.S. van der Goot, "Composition and Crystal Structure of Hexagonal Cu-Rich Rare Earth-Copper Compounds," *Acta Crystallogr. B, 27*(6), 1085-1088 (1971). (Crys Structure; Experimental)

78Bea: B.J. Beaudry and K.A. Gschneidner, Jr., "Preparation and Basic Properties of the Rare-Earth Metals," in *Handbook on the Physics and Chemistry of Rare Earths,* Vol. 1-*Metals,* K.A. Gschneidner, Jr. and L. Eyring, Ed., North-Holland Physics Publishing Co., Amsterdam, 173-232 (1978). (Equi Diagram; Compilation)

80Mie: A.R. Miedema, P.F. de Chatel, and F.R. de Boer, "Cohesion in Alloys - Fundamentals of a Semi-Empirical Method," *Physica B, 100,* 1-28 (1980). (Thermo; Theory)

80Pop: I. Pop, E. Rus, and O. Pop, "Magnetic Susceptibilities and Knight Shifts of the Intermetallic Compounds $NdCu_4$ and $NdCu_5$," *J. Phys. Chem. Solids, 41,* 1315-1318 (1980). (Crys Structure; Experimental)

81Goo: D.A. Goodman, J.W. Cahn, and L.H. Bennett, "The Centennial of the Gibbs-Konovalov Rule for Congruent Points-Its Underlying Theoretical Basis and Its Application to Phase Diagram Evaluation," *Bull. Alloy Phase Diagrams, 2*(1), 29-34 (1981). (Equi Diagram, Thermo; Review)

***83Car:** M.M. Carnasciali, G.A. Costa, and E.A. Franceschi, "Phase Equilibria in the Nd-Cu System," *J. Less-Common Met., 92,* 97-103 (1983). (Equi Diagram, Crys Structure, Thermo; Experimental; #)

83Cha: M.W. Chase, "Heats of Transition of the Elements," *Bull. Alloy Phase Diagrams, 4*(1), 123-124 (1983). (Thermo; Compilation)

83Che: C.S. Cheng and L.-Q. Nong, "A Phase Diagram of the Alloys of the Nd-Cu Binary System," *Acta Phys. Sinica, 32*(11), 1449-1454 (1983) in Chinese. (Equi Diagram, Crys Structure; Experimental; #)

83Nie: A.K. Niessen, F.R. de Boer, R. Boom, P.F. de Chatel, W.C.M. Mattens, and A.R. Miedema, "Model Predictions for the Enthalpy of Formation of Transition Metal Alloys II," *Calphad, 7*(1), 51-70 (1983). (Thermo; Theory)

84Lak: C. Laks, J. Pelleg, and L. Zevin, "Notes on the Nd-Cu System," *J. Less-Common Met., 102,* 23-28 (1984). (Equi Diagram, Crys Structure; Experimental; #)

86Gsc: K.A. Gschneidner, Jr. and F.W. Calderwood, "Intra Rare Earth Binary Alloys: Phase Relationships, Lattice Parameters and Systematics," in *Handbook on the Physics and Chemistry of Rare Earths,* Vol. 8, K.A. Gschneidner, Jr. and L. Eyring, Ed., North-Holland Physics Publishing Co., Amsterdam, 1-161 (1986). (Equi Diagram, Crys Structure; Compilation)

*Indicates key paper.
#Indicates presence of a phase diagram.

Cu-Nd evaluation contributed by **P.R. Subramanian,** Materials Science Division, Universal Energy Systems, Incorporated, 4401 Dayton-Xenia Road, Dayton, OH 45435 and **D.E. Laughlin,** Department of Metallurgical Engineering and Materials Science, Carnegie Mellon University, Pittsburgh, PA 15213. Work was supported by the International Copper Research Association, Inc. (INCRA) and the Department of Energy through the Joint Program on Critical Compilation of Physical and Chemical Data coordinated through the Office of Standard Reference Data, National Bureau of Standards. The authors wish to thank Dr. K.A. Gschneidner, Jr., Director, and F.W. Calderwood, Rare-earth Information Center, Ames Laboratory, Iowa State University, Ames, IA, for providing part of the bibliographic search and the computer program for the critical evaluation of crystallographic data. The authors would also like to thank Dr. D.J. Chakrabarti for his assistance with some of the computer programs and Mr. Pei Shiyou for providing the English translation of [83Che]. Literature searched through 1985. Professor Laughlin is the ASM/NBS Data Program Category Editor for binary copper alloys.

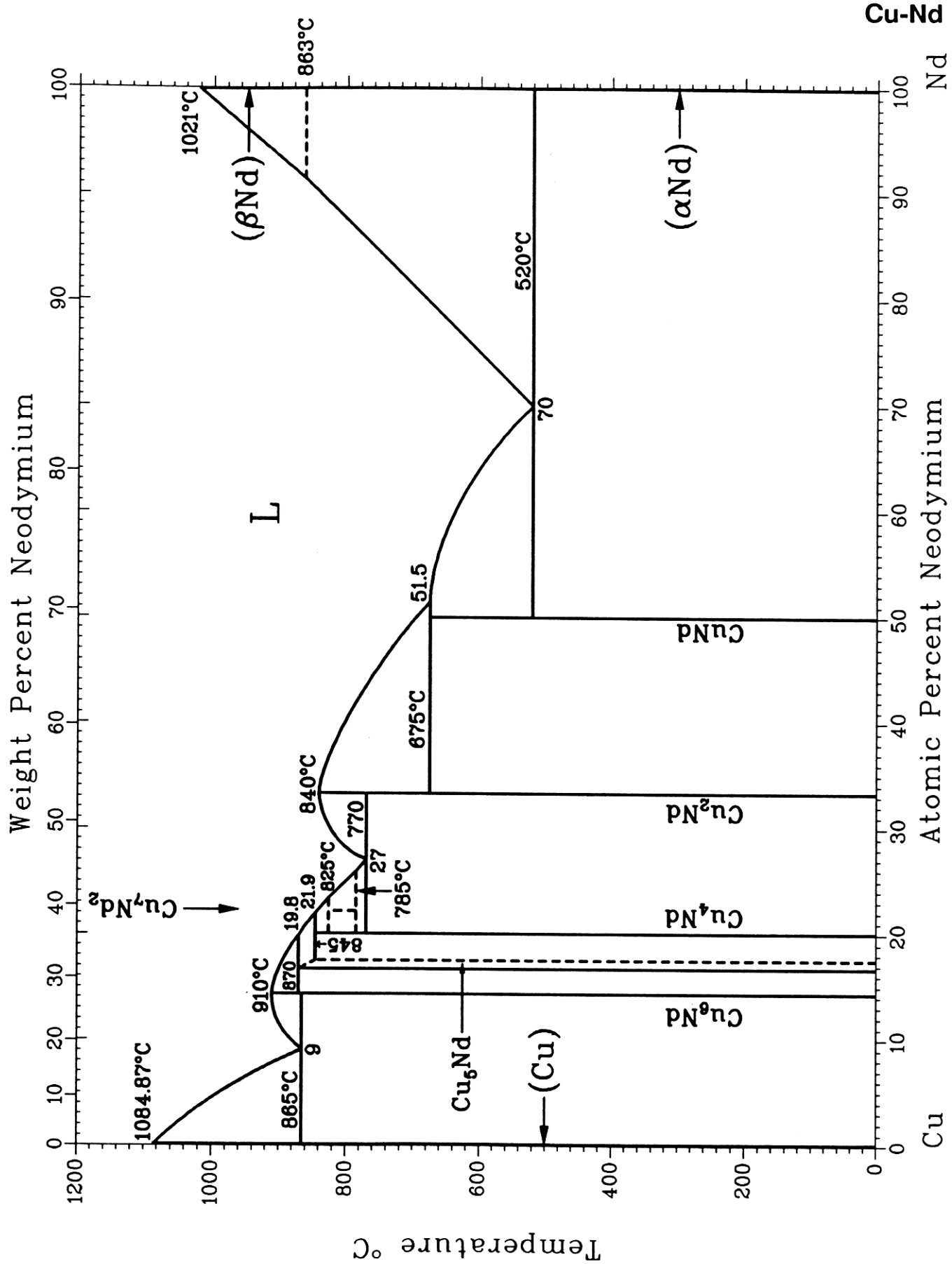

P.R. Subramanian and D.E. Laughlin

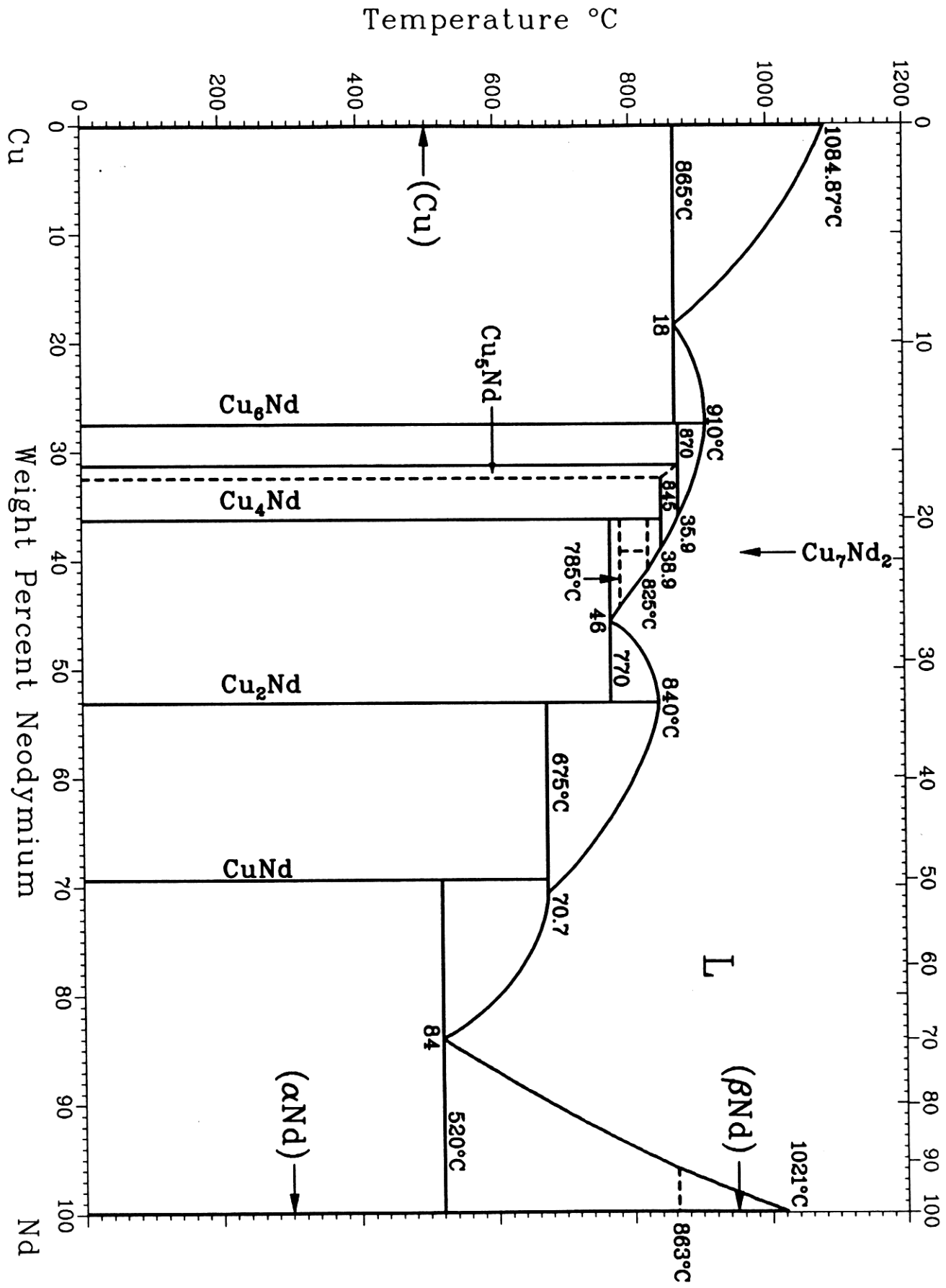

P.R. Subramanian and D.E. Laughlin